electricity

MDPI

Article

Mitigating Grid Congestion: Battery Storage as a Flexible Non-Wire Solution for System Operators Facing Investment Restrictions

Domagoj Badanjak and Hrvoje Pandžić *

University of Zagreb Faculty of Electrical Engineering and Computing, Unska 3, 10000 Zagreb, Croatia; domagoj.badanjak@fer.hr

* Correspondence: hrvoje.pandzic@fer.hr

Abstract

An increasing penetration of distributed energy resources and electrification-driven peak demand pose significant challenges to distribution networks, often resulting in voltage violations and congestion. This paper presents a multi-stage optimization framework that enables battery storage unit (BSU) to act as a flexible non-wire alternative to traditional grid expansions conducted by Distribution System Operators (DSO), but also helpful for Transmission System Operators (TSO). The proposed method integrates a mixed-integer planning model with a quadratically constrained, second-order-cone–relaxed, AC optimal power flow to determine the optimal siting and sizing of battery storage. Representative operating days are obtained through clustering, while the operational optimization model evaluates battery participation in energy and reserve markets under network constraints. The value of flexibility the DSO procures from an independently-owned battery storage unit is determined as the opportunity cost of providing this flexibility as opposed to taking part in the fast reserves and day-ahead energy markets. The results obtained offer valuable information when weighing the decision between network expansion and alternative strategies and determine the price of flexibility that the DSO can offer to an independently owned storage unit. The results confirm that battery storage can defer network investments while providing transparent and economically justified flexibility remuneration. The proposed framework is implemented sequentially, with strong coupling between planning and operational stages through physical constraints and economic signals.

Keywords: battery storage; distribution network; flexibility; congestion management; investment deferral

Check for updates

Academic Editor: Ottorino Veneri

Received: 19 March 2026
Revised: 1 May 2026
Accepted: 3 May 2026
Published: 2 June 2026

Copyright: © 2026 by the authors. Licensee MDPI, Basel, Switzerland. This article is an open access article distributed under the terms and conditions of the Creative Commons Attribution (CC BY) license.

1. Introduction

1.1. Motivation

Distribution networks are traditionally characterized as energy sinks with foreseeable load curves, whose security is achieved by often excessive investments and upgrades. With the process of electrification of other sectors, i.e., heating and transportation, both the peak loads and the overall electricity consumption increases [1]. On the other hand, the ongoing energy transition puts even higher pressure on the distribution networks, which accommodate more and more distributed flexible assets, primarily renewable energy sources (RES), energy storage and demand response resources, jointly referred to as Distributed Energy Resources (DER).

These two processes result in greater uncertainty and higher spread between peaks and valleys of the net load curves in distribution networks, causing extreme voltage levels, both high and low, thermal violations and bidirectional power flows [2]. These issues cannot be effectively solved using the traditional fit-and-forget approach based solely on network upgrades.

Instead, more active approaches based on flexibility provision and coordinated operation of distributed energy resources are required to ensure secure and economically efficient system operation. DERs should be controlled and operated in a way to reduce the need for economically unsound network upgrades, however, they should be appropriately remunerated for such services. Hence, market mechanisms such as the day-ahead market (DAM) and the primary control reserve (PCR) are widely regarded for the model proposed in this paper.

Indeed, Sun et al. argue that shared storage models in PV-ES projects within incremental distribution networks significantly improve investment returns while reducing carbon emissions and increasing renewable energy integration [3]. Legislative bodies strongly encourage Distribution System Operators (DSO) to embrace flexibility procurement methods to secure safe and reliable power supply. At the European Union (EU) level, RePowerEU Plan [4] is one of the latest EU directives that strives to accelerate the energy transition, emphasizing flexibility services and the active role of DSOs.

The main reason for including DERs in distribution network operation is higher efficiency and avoidance of long construction times. It is important to note that the market acts in European countries, e.g., [5,6], forbid the DSOs to own, develop, manage or operate energy storage facilities, with possible exceptions only for rather specific cases. This regulatory constraint shifts the role of the DSO from direct asset ownership to planning and procurement of flexibility services from third-party providers.

This paper develops a methodology that determines the price of providing network services during a limited number of time periods throughout the year. The overall cost of flexibility in the long run should be lower than the network upgrade costs to the DSO, while remaining attractive to the flexibility provider, in this case battery energy storage. As the reservation of capacity and specific operating regimes at specific times limit the battery storage and cause opportunity costs, the DSO needs to at least match the revenue lost in the energy and reserves markets. Procuring flexibility at critical time periods emerges as a rational choice, particularly when such events are infrequent, rendering network expansion financially unsustainable due to its underutilization.

To address this challenge, this paper introduces a structured multi-stage approach from the perspective of a DSO. In the first step, the DSO solves the optimal siting and sizing problem of a battery storage unit that provides flexibility to the network during the hours of need. The second step derives representative days based on a clusterization technique, while the final step solves an operational problem with the primary objective of determining the value of procured flexibility, which can then be offered to profit-oriented players who provide the flexibility services.

1.2. Literature Review

To address the challenges of integration of high share of RES and provide end consumers a secure power supply, DSOs should assess the ability of their network to accommodate new loads and DERs, and investigate the available options to ensure safe and reliable power supply in the coming years.

Hosting capacity is a widely accepted term that denotes the total capacity that can be accommodated in a given network feeder without adversely impacting voltage, protection, and power quality and without the need for feeder upgrades or modifications [7]. Voltage

violations are the dominant limiting factor found in the literature [7,8]. Several papers have been published on this topic, dealing mostly with photovoltaic (PV) and electric vehicle (EV) hosting capacity, generally acknowledging that battery storage increases the hosting capacity [9]. Different authors present various approaches that can generally be divided into deterministic, stochastic, and optimization-based approaches [10].

Deterministic approaches rely on known load and generation values and typically evaluate hosting capacity through iterative simulations. Stochastic approaches incorporate uncertainty through probabilistic modeling techniques [11], most commonly based on Monte Carlo simulations [12,13]. Optimization-based methods rely on solving an optimization problem with an objective function such as maximization of the active power injection of DERs, while ensuring technical and economic constraints are satisfied. The most dominant approaches include AC (and DC) optimal power flow (OPF) [14], particle-swarm optimization [15,16], and genetic algorithms [17].

While these approaches provide valuable insights into network performance and hosting capacity, they predominantly focus on technical optimization and often assume storage units to be owned or controlled by the DSO. Besides observing DERs from the network perspective, it is equally important to observe them from the investors' perspective, as the investment should return the desired yields [18,19].

Investment problems are generally complex and require large amounts of data. Therefore, historical load profiles are often grouped using clustering techniques to reduce computational complexity while preserving accuracy [20–24].

Existing studies provide valuable insights into hosting capacity assessment, battery siting and sizing, and optimization-based network analysis. However, they predominantly focus on technical performance metrics and often assume storage units to be owned or directly controlled by the DSO.

As a result, the economic interaction between market-driven battery operation and distribution network constraints remains insufficiently explored. In particular, limited attention has been given to profit-oriented battery storage units that primarily participate in electricity markets and provide grid support only when economically incentivized. Moreover, existing approaches rarely quantify the economic value of flexibility as an explicit opportunity cost resulting from constrained operation.

To address this gap, this paper proposes a multi-stage optimization framework that links battery storage planning with market-based operation under full AC network constraints. The framework explicitly quantifies the value of flexibility as the difference between unconstrained and network-constrained operation, thereby providing a transparent and practically applicable basis for flexibility procurement in distribution networks.

1.3. Policy and Market Context for Battery-Based Flexibility Provision

The deployment and utilization of battery energy storage systems in distribution networks are strongly influenced by the prevailing policy framework and market design. While the proposed methodology focuses on techno-economic optimization, its practical applicability depends on regulatory conditions that define the roles, responsibilities, and remuneration mechanisms for flexibility providers.

In many regulatory frameworks, Distribution System Operators are restricted from owning and operating storage assets, which requires the procurement of flexibility services from third-party profit-oriented battery operators [25]. This regulatory separation underscores the importance of transparent valuation mechanisms, such as the opportunity-cost-based flexibility assessment proposed in this work.

Market mechanisms also play a critical role in determining the availability of battery flexibility. Day-ahead energy markets and ancillary service markets, such as primary

control reserves, represent the most common revenue streams for battery storage today. Network constraints that limit participation in these markets directly affect investment incentives and operational strategies [26].

Therefore, accurately quantifying the economic impact of network constraints on battery operation is essential for designing effective flexibility procurement mechanisms.

From a policy perspective, the proposed approach supports ongoing regulatory developments aimed at integrating flexibility markets at the distribution level, enabling DSOs to address local congestion through competitive and technology-neutral mechanisms [27].

Overall, the inclusion of policy and market considerations highlights that the effectiveness of battery-based non-wire alternatives is not solely determined by technical feasibility, but also by the alignment between network needs, market incentives, and regulatory constraints.

1.4. Paper Contribution and Structure

This paper proposes a multi-stage optimization framework that links battery storage planning, operation, and market participation under distribution network constraints. Table 1 gives a short comparison of the proposed approach with related studies.

The main contributions of this paper are summarized as follows:

- Optimal siting and sizing of battery storage from a DSO planning perspective under network constraints.
- A market-based operational model including participation in day-ahead and reserve markets.
- A novel definition of flexibility value based on opportunity cost.

Table 1. Comparison of the proposed approach with related studies.

Study	Focus	Network	Market	Flexibility Value
Boonluk et al. (2020) [16]	Siting/sizing	Simpl.	No	Not considered
Gomes & Ferreira (2018) [17]	Hosting cap.	Simpl.	No	Not considered
Pandžić et al. (2018) [18]	Investment	AC	Energy	Implicit
Vicente-Pastor et al. (2019) [28]	TSO–DSO	AC	Flex	Welfare-based
This work	**Plan. + Oper.**	**AC-OPF**	**DAM + PCR**	**Opp. cost**

Unlike most existing studies, the proposed approach explicitly captures the economic interaction between market-driven battery operation and distribution network constraints, providing a transparent basis for flexibility valuation under realistic regulatory conditions.

The rest of the paper is structured as follows. Mathematical formulation of the model is given in Section 2, while the case study and results are presented in Section 3. The final conclusion and further research thoughts are given in Section 4.

2. Mathematical Formulation

The proposed methodology is formulated as a multi-stage optimization problem aimed at determining the optimal siting, sizing, and operation of battery storage units within a distribution network. In the first stage, the objective is to identify the optimal location and capacity of the battery storage system to ensure network feasibility under all operating conditions. The decision variables include the battery location, power rating, and energy capacity, while the constraints are defined by AC power flow equations, voltage limits, and equipment capacity limits. The optimization framework and simulations presented in this study were implemented in the Python programming environment using the Gurobi Optimizer mathematical optimization solver. The optimization problem was solved using the Gurobi Optimizer version 12.0.2 under an academic license for non-commercial research

purposes. Computations were performed on a workstation equipped with an Apple M2 Pro processor running macOS Darwin 25.3.0.

In subsequent stages, the operational behavior of the battery is optimized with and without network constraints to quantify the economic value of flexibility. The objective functions in these stages aim to maximize the battery's market-based revenue while respecting network constraints and technical limitations. A detailed mathematical formulation of the problem is provided in Section 2.2.

2.1. Nomenclature

2.1.1. Sets and Indices

N	Set of nodes, indexed by i and j
T	Set of time steps, indexed by t

2.1.2. Parameters

L	Number of available BSU sites
M	A large constant used in big-M formulations
$P_i^{\text{gen,max}}$	Maximum active power output of generator i (kW)
$P_i^{\text{gen,min}}$	Minimum active power output of generator i (kW)
$Q_i^{\text{gen,max}}$	Maximum reactive power output of generator i (kVAr)
$Q_i^{\text{gen,min}}$	Minimum reactive power output of generator i (kVAr)
R_{ij}	Line resistance between node i and j (Ω)
$U_i^{\max}$	Maximum squared voltage magnitude at bus i (V^2)
$U_i^{\min}$	Minimum squared voltage magnitude at bus i (V^2)
X_{ij}	Line reactance between nodes i and j (S)
$\overline{P}_i$	Maximum charging and discharging power of a BSU at bus i (kW)
$p_{i,t}^{\text{load}}$	Active load at bus i in time period t (kW)
λ_t^{DA}	Day-ahead market price at time t (€/MWh)
λ_t^{PCR}	Primary control reserve price at time t (€/MW)
ϕ	Duration (number of time steps) during which the PCR service remains active
π^{cap}	BSU capacity cost (€/kWh)
π^{ch}	BSU charging power cost (€/kW)
π^{dch}	BSU discharging power cost (€/kW)
$\pi^{\text{ch,fast}}$	BSU fast charging power cost (€/kW)
$\pi^{\text{dch,fast}}$	BSU fast discharging power cost (€/kW)
π^{site}	Fixed cost for establishing a new BSU site (€)

2.1.3. Variables

$c_{i,t}^{\text{DAM}}$	Day-ahead market revenue at bus i at time t (€)
$c_{i,t}^{\text{PCR}}$	Primary control reserve revenue at bus i at time t (€)
$ch_{i,t}$	Charging power of the BSU at bus i at time t (kW)
$ch_{i,t}^{\text{DA}}$	Charging power from DAM for BSU at bus i at time t (kW)
$dch_{i,t}$	Discharging power of the BSU at bus i at time t (kW)
$dch_{i,t}^{\text{DA}}$	Discharging power to DAM for BSU at bus i at time t (kW)
$e_i^{\max}$	Battery capacity of the BSU installed at bus i (kWh)
$i_{ij,t}$	Squared current flow between nodes i and j at time t (A^2)
$n_{i,t}^{\text{fast}}$	Fast charging and discharging power of the BSU at bus i at time t (kW)
$n_{i,t}^{\text{q1}}$	Auxiliary variable for reactive power constraints at bus i at time t
$n_{i,t}^{\text{q2}}$	Auxiliary variable for reactive power constraints at bus i at time t
$p_{ij,t}$	Active power flow from node i to j at time t (kW)
p_i^{batt}	Charging and discharging power of the BSU at bus i (kW)

$p_{j,t}^{\text{gen}}$	Active power generated at bus j at time t (kW)
$p_{i,t}^{\text{PCR}}$	Reserved power for PCR by BSU at bus i at time t (kW)
$q_{ij,t}$	Reactive power flow from node i to j at time t (kVAr)
$q_{j,t}^{\text{batt}}$	Reactive power output of the BSU at bus j at time t (kVAr)
$q_{j,t}^{\text{gen}}$	Reactive power generated at bus j at time t (kVAr)
$soe_{i,t}$	State of energy of the BSU at bus i at time t (kWh)
$u_{j,t}$	Squared voltage magnitude at bus j at time t (V^2)
$x_{i,t}^{\text{DA}}$	Binary variable indicating whether BSU at bus i is charging (1) or discharging (0) at time t
$x_{i,t}^{\text{gen}}$	Binary variable indicating generator status at bus i at time t
x_i^{site}	Binary variable indicating if a BSU is installed at bus i

2.2. Algorithm

The proposed methodology is based on a multi-stage optimization framework designed to support distribution system operators in assessing and mitigating network congestion. In the first stage, a multi-temporal AC optimal power flow is solved without battery support in order to evaluate the feasibility of network operation and to identify congestion-prone periods under realistic load and market price profiles. This baseline assessment allows the detection of critical operating conditions and provides quantitative indicators of voltage and loading violations. Building on this analysis, the second stage addresses the planning aspects of battery deployment from the DSO perspective by solving the optimal siting and sizing problem for battery storage units. This step determines the locations and capacities required to provide effective flexibility support to the network. It should be emphasized that the DSO does not directly invest in or own the battery storage units, but uses the proposed optimization framework to identify optimal locations and required capacities for flexibility procurement from third-party providers. The results also provide insight into the potential commercial viability of battery storage investments and support the design of tendering procedures. To reduce computational complexity in the subsequent operational analysis, a clusterization procedure is applied to identify representative days that capture the dominant network stress patterns. The representative days are used to approximate the full annual operation, where each day is assigned a weight corresponding to its frequency of occurrence, allowing for an accurate estimation of annual results without solving the full time-series problem.

In the final stage, the optimal operational strategy of the battery storage system is derived for each representative day, both with and without network constraints. This stage jointly considers energy arbitrage, reserve provision, and voltage constraints, enabling a direct comparison of system performance and quantification of the value of battery flexibility in alleviating network violations.

The proposed algorithm is illustrated in Figure 1.

Although the methodology is implemented as a sequence of optimization steps, the framework is integrated through the consistent transfer of decisions and constraints between stages. In particular, the planning results define the feasible operational space, while the operational optimization determines the economic value of flexibility, thereby providing a direct link between planning and market-based operation. The proposed approach differs from existing two-stage planning and operation models for battery energy storage in several key aspects. While prior studies typically embed storage siting and sizing within a joint cost-minimization framework—often coupled with demand response programs and primarily applied to meshed network structures—the methodology proposed in this work is explicitly congestion-driven and feasibility-oriented, with a focus on radial distribution networks operating under investment constraints. In particular, a multi-temporal AC opti-

mal power flow is first solved without battery support in order to assess the feasibility of network operation and to identify congestion-prone periods and voltage violations under realistic load and market price profiles. This feasibility-first baseline assessment directly informs subsequent planning decisions and links battery siting and sizing to physically observed network infeasibilities rather than generic economic indicators. Moreover, the operational value of battery flexibility is quantified by deriving optimal battery operation strategies both with and without network constraints. This comparison enables a direct assessment of the contribution of battery storage to congestion mitigation and voltage support, which is not explicitly addressed in conventional two-stage planning models. By focusing on radial distribution grids and DSO-oriented decision-making processes, the proposed framework complements existing approaches that predominantly target meshed networks and market-oriented applications.

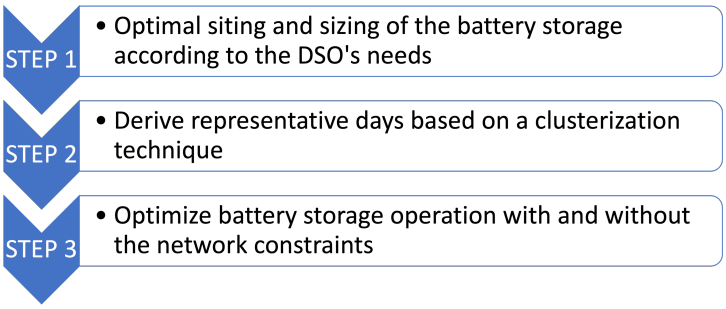


Figure 1. High level steps of the proposed method.

Flexibility is defined as the capability of the battery storage system to deviate from its profit-maximizing operating schedule in order to support network operation under technical constraints. In this work, the value of flexibility is quantified as the corresponding economic opportunity cost, i.e., the difference in achievable profit between unconstrained market-driven operation and network-constrained operation.

The economic model considers day-ahead market (DAM) prices as the primary revenue source for the battery storage system, while reserve services are included as a potential additional market. Reactive power support, however, is not remunerated within the considered framework and is treated as a mandatory service imposed by network constraints. As a result, the provision of reactive power reduces the available capacity for active power dispatch and thus indirectly impacts the battery's market revenue. This effect is captured in the model as part of the opportunity cost associated with flexibility provision.

Model Construction and Theoretical Basis

The proposed framework combines mixed-integer linear programming (MILP) with a multi-temporal AC optimal power flow (AC-OPF) formulation to jointly capture discrete investment decisions, time-coupled battery operation, and nonlinear network constraints. The MILP structure is employed to model battery siting and sizing decisions, operational mode selection, and market participation choices, while the AC-OPF component ensures a physically consistent representation of power flows, voltage magnitudes, and line loading within the distribution network. Thus, the resulting models are mixed-integer quadratically constrained problems. The AC network model is based on a multi-period branch-flow formulation, which explicitly represents active and reactive power balances, voltage magnitude limits, and thermal constraints on network elements. This formulation preserves the essential nonlinear characteristics of distribution system operation while remaining computationally tractable for the considered planning horizon. Time coupling is introduced through the battery state-of-energy dynamics [29], which link consecutive time steps and ensure physically meaningful charging and discharging trajectories. Binary

decision variables are used to enforce mutually exclusive operational modes (charging, discharging, reserve provision) and to represent discrete siting decisions. Continuous variables capture power flows, voltages, and energy states. Big-M formulations are applied where necessary to link binary and continuous variables, with parameter values chosen conservatively to avoid numerical instability. Model accuracy and reliability are ensured through (i) the use of physically grounded AC power flow constraints rather than simplified DC or linearized network models, (ii) explicit enforcement of voltage and thermal limits in all time steps, and (iii) consistent temporal alignment of load and market price data. Solver convergence and feasibility are systematically verified for each simulation run, and infeasible cases are explicitly identified and analyzed. The overall framework can be interpreted as a coupled MILP–AC-OPF formulation, where discrete planning and operational decisions are integrated with continuous network constraints. In the planning stage, binary variables determine battery siting and sizing, while the AC-OPF constraints ensure network feasibility. In the operational stage, the resulting battery configuration is used to evaluate market participation and flexibility provision under network constraints. This sequential coupling ensures consistency between planning decisions, network physics, and market-based operation.

2.3. Model Verification and Consistency Checks

To verify the correctness and reliability of the proposed optimization framework, a set of consistency and validation checks was performed using historical load and market data. The objective of this verification is not short-term price or load prediction, but rather to ensure that the model produces physically and economically plausible operating decisions under realistic system conditions. First, the base-case operation without battery support was evaluated for all considered days. The resulting infeasible periods, characterized by voltage violations or line overloads, were found to coincide with historically observed high-load conditions and peak-demand intervals. This confirms that the model correctly identifies stress conditions in the distribution network. Second, when battery storage is enabled, the optimization results were verified to satisfy all AC network constraints, including voltage magnitude limits and line thermal ratings, across all time steps. The resulting voltage profiles and power flows remain within acceptable operational ranges, demonstrating that the AC-OPF formulation enforces physically consistent behavior. Third, the optimal battery operation patterns—charging during low-price periods and discharging or providing reserves during high-price or network-constrained periods—are consistent with established operational principles and observed battery dispatch behavior in existing market-based storage applications. Finally, sensitivity analyses with respect to battery size, power rating, and economic parameters further confirm the robustness of the model outcomes. Small variations in input parameters lead to smooth and interpretable changes in the optimization results, indicating numerical stability and structural consistency of the formulation.

2.3.1. Step 1: Optimal Siting and Sizing of Battery Storage

In the first step the DSO finds optimal BSU location(s) and size(s) to ensure feasible power flows within its network at all times at minimum cost. The branch-flow model [30,31] is used to model the AC optimal power flow (OPF). To find the most cost-efficient BSU investment option while complying with all technical constraints, we run as many daily optimization problems as there are critical days for the DSO in the input data.

The most important factors that affect the investment size are the number of locations where BSUs can be installed and their characteristics (power and energy capacity). Hence, the objective function minimizes the number of potential locations (x^{site}), as each location

incurs a lump investment cost, π^{site}, independent of the battery capacity (this lump cost may include grid connection fees, project documentation, etc.), and battery installation cost, $batt^{\text{cost}}$, that depends on its energy and power capacity. Equation (2) defines the BSU installation cost, where π^{cap} is the cost of a unit of energy capacity, π^{ch} is the cost of a unit of charging power, whereas π^{dch} is the cost of a unit of discharging power. Additionally, we penalize excessive charging and discharging power rates, meaning that each additional unit of charging or discharging power, which results in high C-rate, is penalized using factor π^{fast}. $e_i^{\max}$ is a variable that determines the battery capacity, whereas p_i^{ch} and p_i^{dch} denote the battery storage maximum charging and discharging powers. Constraints (3) and (4) define the battery charging power exceeding a specific C-rate, e.g., C-rate above 1, for the charging and the discharging directions. The set of decision variables is: $\sigma = \{ x^{\text{site}}, batt_i^{\text{cost}}, e_i^{\max}, p_i^{\text{batt}}, n_{i,t}^{\text{fast}}, p_{ij,t}, i_{ij,t}, p_{j,t}^{\text{gen}}, q_{ij,t}, q_{i,t}^{\text{gen}}, q_{i,t}^{\text{batt}}, u_{i,t}, x_{i,t}^{\text{gen}}, soe_{i,t}, x_{i,t}^{\text{batt}}, ch_{i,t}, dch_{i,t}, p_{i,t}^{\text{PCR}} \}$.

$$\min_{\sigma} \sum_{i=1}^{N} [\pi^{\text{site}} \cdot x_i^{\text{site}} + batt_i^{\text{cost}}] \tag{1}$$

where

$$batt_i^{cost} = \pi^{\text{cap}} \cdot e_i^{\max} + \pi^{\text{pow}} \cdot p_i^{\text{batt}} + \pi^{\text{fast}} \cdot n_i^{\text{fast}}, \quad \forall i \tag{2}$$

$$n_i^{\text{fast}} \geq p_i^{\text{batt}} - e_i^{\max}, \quad \forall i \tag{3}$$

$$n_i^{\text{fast}} \geq 0, \quad \forall i \tag{4}$$

Constraint (5) limits the maximum number of nodes where the potential BSUs may be installed to a user-predefined parameter L. x_i^{site} is a binary variable whose value denotes if a specific node hosts a BSU (value 1) or not (value 0). Constraint (6) determines the energy capacities at locations where the BSUs are installed.

$$\sum_{i=1}^{N} x_i^{\text{site}} \leq L, \tag{5}$$

$$e_i^{\max} \leq M \cdot x_i^{\text{site}}, \quad \forall i \tag{6}$$

Constraint (7) models active power flow between the nodes. $p_{ij,t}$ denotes active power flow between nodes $i - j$ during time period t, while $i_{ij,t}$ is the squared current between those nodes and R_{ij} is the line resistance. Variable $p_{i,t}^{\text{gen}}$ represents active power output from a generator located at node j (if any), whereas parameter $P_{j,t}^{\text{load}}$ depicts the demand at node j during time period t. Variables $dch_{j,t}$ and $ch_{j,t}$ represent the battery discharging and charging at node j during time period t. Term $\sum P_{jm,t}$ denotes power flows between node j and the neighbouring nodes. Constraint (8) models reactive power flow in an analogous manner as Constraint (7) does for active power flow. Reactive power generation and battery input through an inverter are variables, while the reactive demand is a parameter.

$$\begin{aligned} p_{ij,t} = R_{ij}\, i_{ij,t} - \left(p_{j,t}^{\text{gen}} + dch_{j,t} - p_{j,t}^{\text{load}} - ch_{j,t} \right) \\ + \sum_{m:j \to m} p_{jm,t}, \quad \forall (i,j),\, t \end{aligned} \tag{7}$$

$$\begin{aligned} q_{ij,t} = i_{ij,t} \cdot X_{ij} - (q_{j,t}^{\text{gen}} - q_{j,t}^{\text{load}} + q_{j,t}^{\text{batt}}) + \\ \sum_{m:j \to m} Q_{jm,t}, \quad \forall ij, t \end{aligned} \tag{8}$$

Constraint (9) models nodal voltages, where $u_{i,t}$ represents the squared voltage.

$$u_{j,t} = u_{i,t} - 2(R_{ij} \cdot p_{ij,t} + X_{ij} \cdot q_{ij,t}) + i_{ij}(R_{ij}^2 + X_{ij}^2), \quad \forall ij, t \tag{9}$$

Constraint (10) in the exact formulation should be an equality which connects the current, the voltage and the power. Since such formulation would be non-convex, it is relaxed in the form of a rotated second-order cone constraint [32].

$$i_{ij,t} \cdot u_{i,t} \geq p_{ij}^2 + q_{ij}^2, \quad \forall ij, t \tag{10}$$

Constraints (11)–(13) define the allowed ranges for active and reactive power generation and allowed nodal voltages.

$$P_i^{\text{gen,min}} \cdot x_{i,t}^{\text{gen}} \leq p_{i,t}^{\text{gen}} \leq P_i^{\text{gen,max}} \cdot x_{i,t}^{\text{gen}}, \quad \forall i, t \tag{11}$$

$$Q_i^{\text{gen,min}} \leq q_{i,t}^{\text{gen}} \leq Q_i^{\text{gen,max}}, \quad \forall i, t \tag{12}$$

$$U_i^{\text{min}} \leq u_{i,t} \leq U_i^{\text{max}} \quad \forall i, t \tag{13}$$

The BSU state-of-energy is modeled in Equation (14) using variable $soe_{i,t}$, which represents the state-of-energy of a BSU at node i, while parameter η indicates the battery charging and discharging efficiency.

$$soe_{i,t} = soe_{i,t-1} - (dch_{i,t} \cdot \frac{1}{\eta} + ch_{i,t} \cdot \eta) \cdot \Delta t \quad \forall i, t \tag{14}$$

Constraint (15) limits the BSU's maximum charging power, whereas Constraint (16) limits the BSU's maximum discharging power. p_i^{ch} and p_i^{dch} are variables as the goal in this step is to calculate the optimal BSU charging and discharging capacities in addition to the BSU optimal locations and energy capacities.

$$p_i^{\text{batt}} \cdot x_{i,t}^{\text{batt}} \geq ch_{i,t}, \quad \forall i, t \tag{15}$$

$$p_i^{\text{batt}} \cdot (1 - x_{i,t}^{\text{batt}}) \geq dch_{i,t}, \quad \forall i, t \tag{16}$$

Constraint (17) limits the minimum and maximum state-of-energy of each BSU.

$$k \cdot e_i^{\text{max}} \leq soe_{i,t} \leq e_i^{\text{max}}, \quad \forall i, t \tag{17}$$

A BSU combined with an adequate inverter may provide both active and reactive power to the system, hence Constraints (18) and (19) limit the apparent power that may be provided by a BSU (i.e., its inverter) including charging power, discharging power, reactive power and the power reserved for the PCR. q^{batt} may be positive or negative, as reactive service can be offered in both inductive and capacitive modes,

$$(p_i^{\text{batt}})^2 \geq (ch_{i,t} + p_{i,t}^{\text{PCR}})^2 + (q_{i,t}^{\text{batt}})^2, \quad \forall i, t \tag{18}$$

$$(p_i^{\text{batt}})^2 \geq (dch_{i,t} + p_{i,t}^{\text{PCR}})^2 + (q_{i,t}^{\text{batt}})^2, \quad \forall i, t \tag{19}$$

2.3.2. Step 2: Deriving Representative Days

In the first step, the optimization algorithm is run for every day from the historical data to find the optimal BSU investment that serves the DSO's needs. A clustering method is utilized to prepare the data for the second step – determining the value of flexibility. Each

group consists of n days and a representative day from each group is then used as input for the optimization algorithm in the third step. Python library scikit-learn [33] is used to perform the K-medoids algorithm. The algorithm clusters the data by separating samples in n groups of equal variance, minimizing a criterion known as the inertia or within-cluster sum-of-squares [34]. In contrast to the K-means algorithm, actual data point is the center point (medoid) of a cluster. In order to capture daily load profile representatives that reflect conditions of the observed distribution network in a holistic manner, active and reactive power for all nodes are taken as separate features per hour to form a daily load profile.

Note that this step may be omitted and Step 3 can be run for each day for each day of the year. Step 2 may be used to reduce the computational burden of the presented process.

2.3.3. Step 3: Determining the Value of Flexibility

Based on the optimal battery investment plan calculated in the first step and clustering of the daily load profiles into groups of the representative days in the second step, the third step determines the value of flexibility that a BSU operator provides to the DSO. Each representative day is assigned a weight factor that reflects the number of actual days it represents within the year. The full year, consisting of 365 days, is grouped into clusters of days with similar network characteristics. Each group is represented by one representative day, and its weight indicates how many days from the year share those characteristics. Having battery sites and sizes as parameters, the goal is to determine a fair compensation a DSO would need to pay to a BSU operator. The value of flexibility provided to the DSO is determined as a difference between the BSU operator's profits from participating in the day-ahead and the primary control reserve (PCR) provision markets with and without obeying the network constraints. That is, this optimization algorithm is first run without the network constraints to determine the potential profit, and then with network constraints. The difference in the BSU profit between the former and the latter represents the lost opportunity cost, which the DSO should compensate to the BSU operator. Decision variables are the BSU's activity, whereas the BSU locations and capacities are parameters calculated in the first step. Hence, Constraints (20)–(29) are valid for the network unaware case, and Constraints (7)–(14) need to be added when considering the network constraints. The set of decision variables is: $\zeta = \{c_{i,t}^{\mathrm{DAM}}, ch_{i,t}^{\mathrm{DA}}, dch_{i,t}^{\mathrm{DA}}, c_{i,t}^{\mathrm{PCR}}, p_{i,t}^{\mathrm{PCR}}, x_{i,t}^{\mathrm{DA}}, soe_{i,t}^{\mathrm{PCR}}, soe_{i,t}\}$.

Objective function (20) maximizes the profit of participating in the day-ahead and primary reserve markets, i.e., DAM and PCR, with λ_t^* denoting hourly prices for respective markets.

$$\max_{\zeta} \sum_{t}^{T} \sum_{i}^{I} [c_{i,t}^{\mathrm{DAM}} + c_{i,t}^{\mathrm{PCR}}] \tag{20}$$

subject to

$$c_{i,t}^{\mathrm{DAM}} = (dch_{i,t}^{\mathrm{DA}} - ch_{i,t}^{\mathrm{DA}}) \cdot \lambda_t^{\mathrm{DA}}, \quad \forall i, t \tag{21}$$

$$c_{i,t}^{\mathrm{PCR}} = p_{i,t}^{\mathrm{PCR}} \cdot \lambda_t^{\mathrm{PCR}}, \quad \forall i, t \tag{22}$$

Constraints (23) and (24) limit the maximum discharging and charging power in the DAM, considering binary variable $x_{i,t}^{\mathrm{DA}}$, which determines if the BSU is in the charging or the discharging mode, and the maximum allowed battery power.

$$dch_{i,t}^{\mathrm{DA}} \leq \overline{\mathrm{P}}_i \cdot x_{i,t}^{\mathrm{DA}} \quad \forall i, t \tag{23}$$

$$ch_{i,t}^{\mathrm{DA}} \leq \overline{\mathrm{P}}_i \cdot (1 - x_{i,t}^{\mathrm{DA}}) \quad \forall i, t \tag{24}$$

As for the PCR, the energy reserved for potential provision of the service at power $p_{i,t}^{\mathrm{PCR}}$ is modelled in (25)–(27). Equation (25) calculates the amount of SOE reserved for PCR activation, while Constraints (26) and (27) further limit the SOE to be used in the day-ahead market considering the possible PCR activated energy. Parameter ϕ represents the time horizon in which the service is activated, e.g., quarter of an hour, and provides the required energy capacity for the PCR provision.

$$soe_{i,t}^{\mathrm{PCR}} = \phi \cdot p_{i,t}^{\mathrm{PCR}} \quad \forall i, t \tag{25}$$

$$soe_{i,t}^{\mathrm{PCR}} + soe_{i,t} \leq e_i^{\max} \quad \forall i, t \tag{26}$$

$$soe_{i,t} - soe_{i,t}^{\mathrm{PCR}} \geq 0 \quad \forall i, t \tag{27}$$

As the PCR provision may be activated in both directions within one time period, the maximum battery power to be utilized is:

$$ch_{i,t}^{\mathrm{DA}} + p_{i,t}^{\mathrm{PCR}} \leq \overline{\mathrm{P}}_i \quad \forall i, t \tag{28}$$

$$dch_{i,t}^{\mathrm{DA}} + p_{i,t}^{\mathrm{PCR}} \leq \overline{\mathrm{P}}_i \quad \forall i, t \tag{29}$$

Constraints (14)–(19) are necessary in all cases, but with an important note that in the second step, the battery location, capacity and power ratings are parameters, whereas constraints (7)–(13) are used for the case when obeying the network constraints. For the sake of clarity, Table 2 show which constraints are used in each of three specific cases: (i) Step 1 (S1), (ii) Step 3 without network constraints (S3-U) and (iii) Step 3 with network constraints (S3-N).

Table 2. Constraint usage across steps.

ID	Constraint	S1	S3-U	S3-N
(1)	Investment objective	✓	–	–
(2)	Battery cost function	✓	–	–
(3)–(4)	Fast C-rate penalty	✓	–	–
(5)	Max BSU installations	✓	–	–
(6)	Capacity if installed	✓	–	–
(7)	Active power flow	✓	–	✓
(8)	Reactive power flow	✓	–	✓
(9)	Voltage drops	✓	–	✓
(10)	SOC relaxation	✓	–	✓
(11)	Generator P limits	✓	–	✓
(12)	Generator Q limits	✓	–	✓
(13)	Voltage bounds	✓	–	✓
(14)	SOE dynamics	✓	✓	✓
(15)–(16)	Charge/discharge limits	✓	✓	✓
(17)	SOE bounds	✓	✓	✓
(18)–(19)	Apparent power limits	✓	✓	✓
(20)	Revenue loss objective	–	✓	✓
(21)–(22)	DAM, PCR revenues	–	✓	✓
(23)–(24)	DAM constraints	–	✓	✓
(25)–(27)	SOE reserve for PCR	–	✓	✓
(28)–(29)	Power rating limits	–	✓	✓

2.4. Simulation Platform and Optimization Workflow

All numerical experiments were executed on a macOS workstation running macOS 15.6.1, equipped with an Apple M2 Pro processor and 16 GB of RAM. The optimization framework was implemented in Python 3.11, while all optimization problems were formulated and solved using the Gurobi Optimizer. version 12.0.2 under an academic license for non-commercial research purposes.

3. Case Study

The case study is conducted on a modified 15-bus radial distribution network, whose data are available in [35]. The network configuration is given in Figure 2. One-year historical DAM prices provided in Figure 3 were fetched from the Croatian Power Exchange (CROPEX [36]) for year 2021, whereas the balancing market prices were calculated according to the currently active Croatian legislative. In the Croatian electricity market the power exchange and system operator apply a common balancing price to all balancing-responsible parties. For each 15-min settlement interval the system operator compares the aggregate generation and demand and establishes whether the power system is short of energy (a positive imbalance) or has a surplus (a negative imbalance). The balancing price is then computed by taking the market price from the day-ahead auction on CROPEX and comparing it to the average price of the balancing energy that was actually activated. If there is a surplus of energy, the settlement price is set equal to the lower of the day-ahead price and the weighted average price of the balancing energy. On the other hand, if there is a shortage, the settlement price is set equal to the higher of these values. This approach rewards participants whose deviations support the system balance and penalises those that aggravate it. A neutralising coefficient is determined so that the total revenue from imbalance payments covers the cost of the balancing energy, and this coefficient is set to zero whenever the weighted average price of balancing energy is negative [37]. A noticeable increase in the DAM prices in the last quarter of the year is due to a combination of factors. Namely, the demand has soared as the effect of the post-pandemic recovery, lower production from RES and a worldwide global energy crisis [38].

The daily load profile of the distribution network was randomly generated using the real data [35] as the base and following the general yearly load trend as seen in many coastal places throughout the Republic of Croatia. Figure 4 presents the annual load in year 2021. The highest peaks occur during the summer time, whereas the distribution network is under the minimum loading conditions during the spring and autumn.

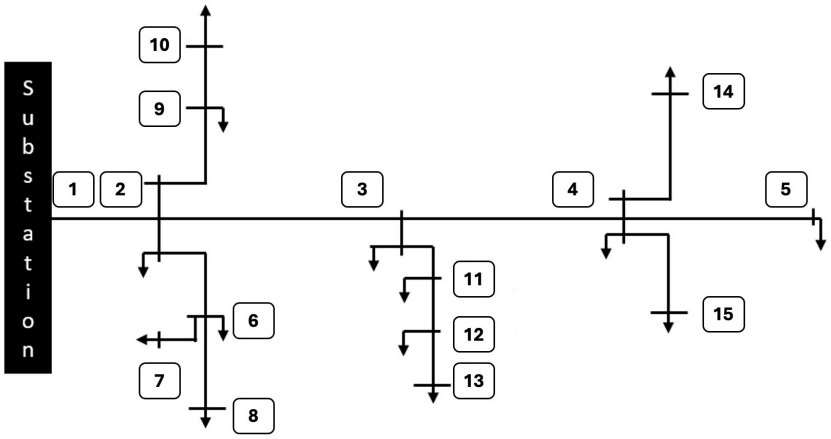


Figure 2. Radial distribution network.

For the battery round-trip efficiency, denoted by η, a value of $\eta = 0.9$ is assumed, reflecting typical performance of battery energy storage systems. The efficiency is incor-

porated into the state-of-energy balance, where charging and discharging processes are adjusted accordingly. Additional internal consumption of the battery system is not explicitly modeled and is considered to be implicitly captured within the efficiency parameter.

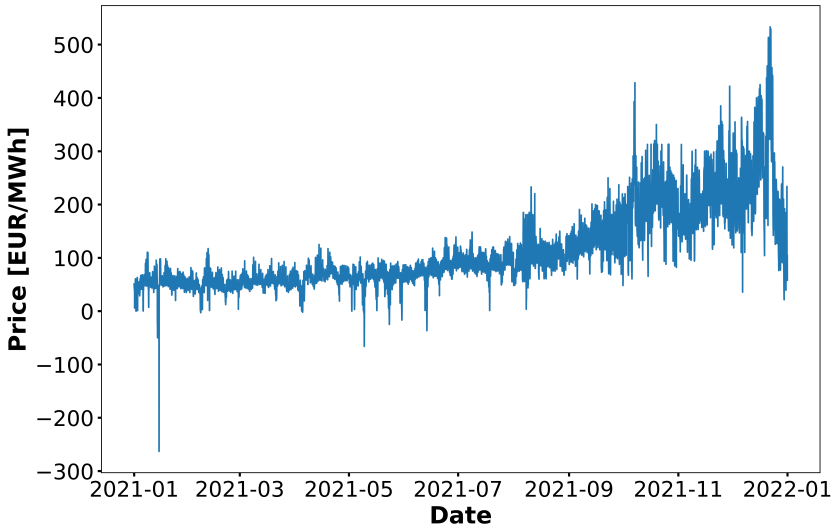


Figure 3. DA prices.

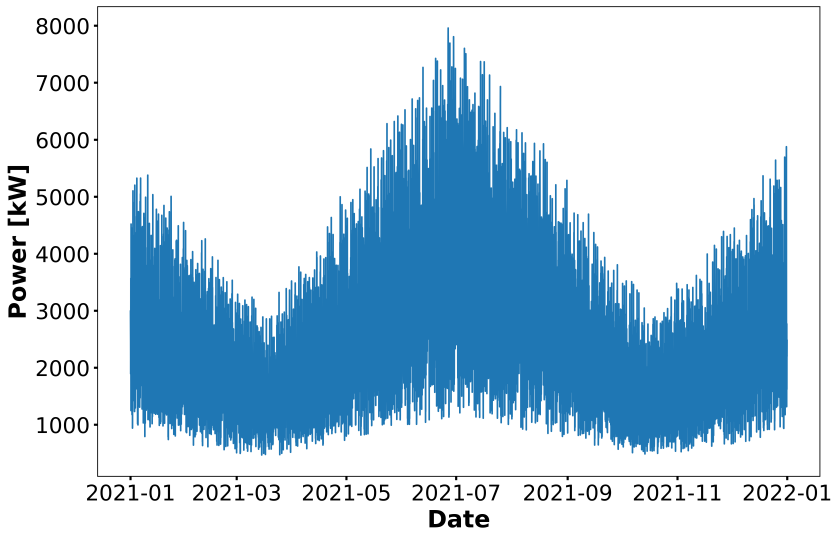


Figure 4. Sum of the loads in the distribution network throughout the observed year.

3.1. First Step—Optimal Battery Location and Sizing

The algorithm was executed for each of the 365 days in 2021. As a result, bus 4 was identified by the DSO as the optimal node for installing a new BSU. In practical terms, this means that for a subset of days the power flow problem would not be feasible without either installing a BSU or opting for a network expansion strategy. Figure 5 illustrates the daily load profile at bus 4 across different months of 2021. The figure clearly shows that the highest peaks occur during summer afternoons, reaching values almost four times greater than the lowest recorded loads.

A detailed analysis further validates these findings. The potential BSU location at bus 4 is situated downstream in the feeder, though not at its most remote point. This choice is driven by the fact that buses 14 and 15 experience considerably higher loads, with peaks approximately two and five times greater than those at bus 4, respectively. On the other hand, the most downstream bus (number 5) has a relatively modest load, comparable in magnitude to that of bus 4. As a result, bus 4 effectively serves as an auxiliary support point

for the heavily loaded neighboring buses 14 and 15. To provide additional perspective, Figure 6 presents the daily load profiles for bus 5.

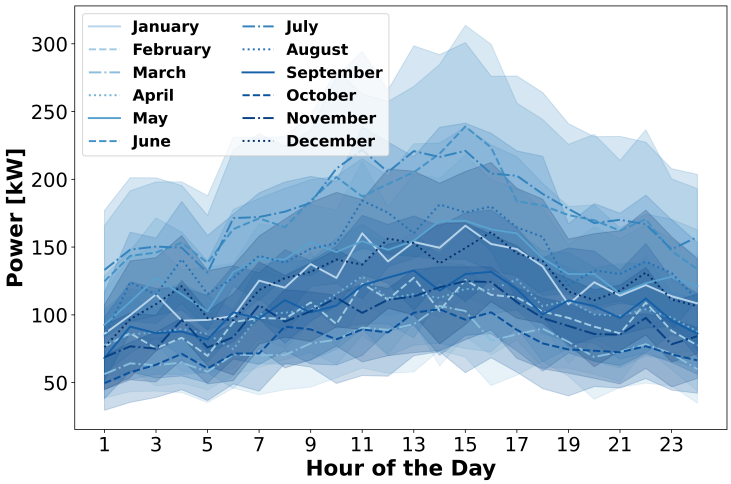


Figure 5. Daily load profiles at bus 4.

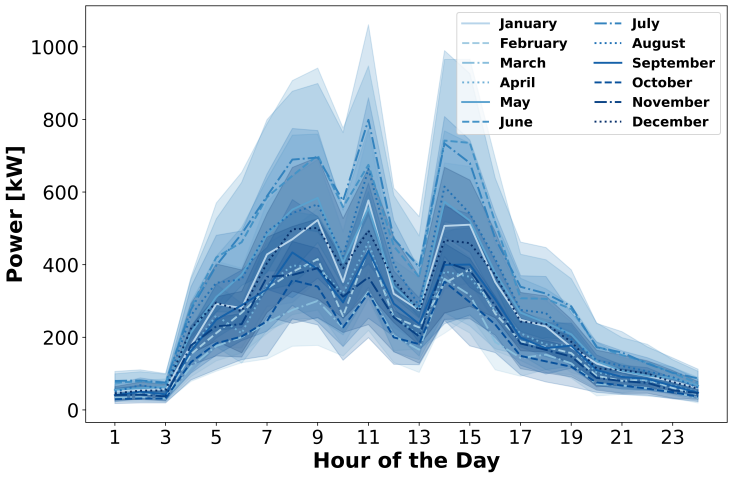


Figure 6. Daily load profiles at bus 5.

To ensure a safe and reliable power supply within the observed distribution network, the model indicates that the BSU should be sized at 13.7 MWh of energy capacity with a rated power of 5 MW.

The year-long feasibility analysis reveals that of the 365 days examined, 115 were classified as *critical*, meaning that the optimization problem would not have been feasible without operating the battery in the charging or discharging mode. Across all days, a total of 355 infeasible hours were identified, corresponding to situations where load demand could not be met without the support of storage. On average, each critical day exhibited nine infeasible hours, ranging from a single hour to extended intervals lasting up to seven consecutive infeasible hours. The main cause of infeasibilities were undervoltages in the observed area.

The temporal distribution of infeasibility is highly seasonal. Summer months dominate the statistics, with June, July, and August together accounting for 298 h, or more than four fifths of the annual total. July alone contributes with critical 152 h, followed by 120 h in June and 26 h in August. In spring, 39 h were observed, almost entirely concentrated in May, while winter shows only 17 h scattered across January and December. Autumn is practically negligible, with just a single infeasible hour in September and no critical events

in October or November. This pattern clearly highlights summer as the period of highest operational stress, driven by the pronounced load and generation mismatches.

A closer look at the time of the day further refines this picture. Infeasibility occurs only sporadically at night, with just six hours between midnight and five in the morning. During the morning ramp (6:00–11:00), the frequency of critical hours increases sharply, accounting for about 120 h. The highest concentration occurs between midday and early afternoon (12:00–17:00), where 142 h are recorded. The absolute peak is found between 14:00 and 15:00, with 92 h over the year. The evening period (18:00–23:00) contributes another 87 h.

Finally, the structure of infeasibility events reveals that they often cluster into consecutive hours within a day, rather than appearing as isolated occurrences. In fact, more than two thirds of all infeasible hours occur in blocks of at least three consecutive hours. In many cases, these events also extend across consecutive days, forming so-called neighbor runs. Over the year, 11 distinct neighbor runs were identified, with the longest lasting 4 consecutive days. This clustering demonstrates that infeasibility is typically a result of sustained stress periods where demand and flexibility are systematically misaligned, rather than short-lived anomalies.

In summary, while infeasibility affects just over ten percent of the days in the year, these events are concentrated in summer and typically manifest as multi-hour and sometimes multi-day blocks. This underscores the importance of battery systems not only as marginal balancing assets but as critical infrastructure for ensuring system feasibility during prolonged stress conditions.

The analysis of the base case reveals that voltage violations are the primary driver of infeasible operating conditions in the network. In total, 355 infeasible hours were identified, corresponding to approximately 4.05% of annual operation, and distributed across approximately 115 critical days. These violations typically occur outside the acceptable voltage range of 0.95–1.05 p.u., with observed values approaching the imposed limits of 0.90–1.10 p.u. The inclusion of the optimally placed BSU significantly improves voltage regulation by providing active power support at critical nodes. This results in a complete elimination of infeasible operating conditions, corresponding to a 100% reduction in voltage violations and infeasible hours. In addition, the number of affected nodes and hours is reduced from widespread violations across the network to fully compliant operation within acceptable voltage limits. From a system perspective, this corresponds to a substantial improvement in voltage stability, as the battery effectively mitigates both undervoltage and overvoltage conditions during peak stress periods.

3.2. Second Step—Clustering

K-means clustering is applied to group daily operating profiles based on load and generation patterns. Each day is represented by a vector of time-series values (e.g., load and generation over 24 h), and the clustering algorithm partitions these profiles into a predefined number of clusters. Each cluster is then represented by a centroid, which serves as a representative day in the subsequent optimization stage.

The number of clusters is selected as a compromise between computational efficiency and the ability to accurately represent system variability. A larger number of clusters increases accuracy but also computational burden, while a smaller number may overlook important operating conditions. The chosen clustering configuration ensures that both typical and critical operating conditions are adequately captured.

The infeasibility analysis has demonstrated that operational stress in the network is not evenly spread across the year but is highly concentrated in specific seasons, times of day, and multi-hour blocks. Most of these events occurred during the summer months, with July alone accounting for more than 40% of all infeasible hours. To ensure that these

recurring stress conditions are adequately represented in the analysis, while at the same time reducing the computational burden of solving optimization problems for every single day of the year, a clustering approach is applied to the daily load profiles.

In this case study, a dataset of 365 daily load profiles was considered for the 15-bus radial distribution network, including both active and reactive power. Even for a modest-sized network such as this, the scale of the data is substantial: more than ten thousand daily load curves arise when considering a year of operation across all buses. Figure 7 illustrates this volume of the data. Directly applying optimization to the full dataset would be computationally demanding and, for larger systems, potentially infeasible.

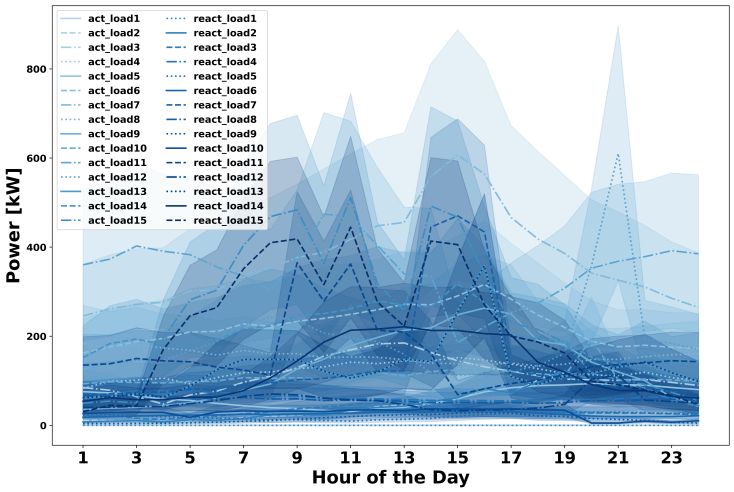


Figure 7. Daily load profiles for all nodes.

To address this challenge, the K-medoids clustering algorithm was used to group the daily load profiles into a smaller number of representative days. Each representative day captures the main temporal and seasonal characteristics of the original dataset while reducing the dimensionality of the problem. The optimal number of clusters was determined using the elbow method [39]., as illustrated in Figure 8. The "elbow" appears at four clusters, indicating that four representative days provide a good balance between the accuracy and the computational tractability.

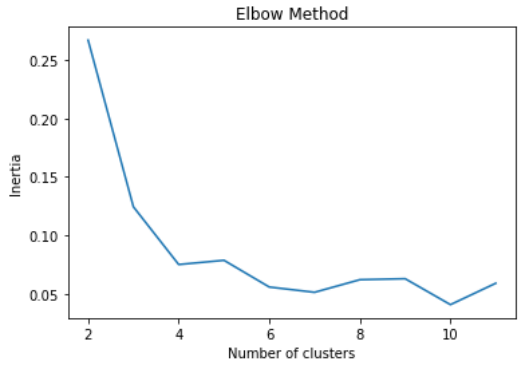


Figure 8. Determining the optimal number of clusters using the elbow method.

A natural question arises: why are all 365 days used for clustering, rather than only the 39 critical days identified earlier? The reason is that clustering aims to provide a set of representative operating conditions for the entire year, not only the extreme cases. By restricting the dataset to critical days only, the resulting clusters would overweight the most stressed conditions and neglect normal or mild operating periods, which are equally relevant for system planning and operation. For example, system investments sized only

for critical days might lead to unnecessary oversizing, while ignoring the majority of benign days where operational flexibility is less demanding. By clustering the full annual dataset, the resulting representative days include both normal and critical conditions in their correct proportion. This ensures that seasonal and temporal diversity is preserved and that optimization results remain realistic for long-term operation.

Another important reason for using the entire 365-day dataset is related to the subsequent economic analysis of flexibility. In order to properly evaluate the value of flexibility, one must also account for those days where the system is not stressed and therefore flexibility has little or no value. Including such days allows for a fair comparison of annual revenues, costs, and the overall profitability of the proposed algorithm. If clustering were restricted only to critical days, the resulting profitability assessment would be artificially inflated, since it would only reflect periods when flexibility is essential, while ignoring times when it provides no additional benefit. The full-year clustering therefore ensures a balanced and comprehensive basis for evaluating both technical feasibility and the economic performance of flexibility resources.

Importantly, the clustering process not only captures typical operating days but also ensures that critical stress periods are represented. One of the four clusters corresponds predominantly to summer days with very high afternoon peaks, which are directly associated with the infeasibility events identified earlier. The other clusters represent spring shoulder days, relatively mild autumn and winter profiles, and transitional days with moderate load variability. Each cluster carries a weight equal to the number of days it represents: cluster 1 corresponds to 109 days, cluster 2 to 57 days, cluster 3 to 81 days, and cluster 4 to 118 days. Together, they sum to the full set of 365 days.

This approach ensures that subsequent optimization tasks can focus on four representative operating conditions while still preserving the essential seasonal variability, capturing both stressed and unstressed periods, and allowing for a meaningful evaluation of technical feasibility and the economic value of flexibility. It is important to distinguish between the roles of full-year analysis and clustering within the proposed framework. In the first step, all 365 days are considered to ensure that battery siting and sizing decisions are robust and account for all possible operating conditions, including extreme scenarios. In contrast, clustering is applied only in the third step, where the computational burden is significantly higher due to the inclusion of market participation and time-coupled operational constraints. Applying clustering in the planning stage could lead to underestimation of critical conditions and result in suboptimal sizing decisions. Therefore, the proposed approach balances robustness in planning with computational efficiency in operational analysis.

3.3. Third Step—Determining the Value of Flexibility Under Grid Constraints

In the final analysis, the location and rated capacity of the BSU are assumed to be predefined. The objective is to determine the optimal operational strategy for the BSU while quantifying the value of flexibility it offers to the DSO.

In both the unconstrained and constrained problems, the BSU participates in the DAM and the PCR market, thereby generating revenue from both energy arbitrage and system frequency support services. However, when network constraints are enforced, the BSU may not be able to deliver the PCR service or even the desired day-ahead power at specific hours. To obey the network constraints, the BSU can either reduce the amount of power injected or subtracted from the network, or inject or subtract reactive power, which may limit its power possibilities due to apparent power limitations. Since reactive power support is not financially compensated in the current market structure, this requirement effectively reduces the available capacity for revenue-generating actions, potentially reducing the profit. This effect is captured through the apparent power limits of the battery inverter. When

reactive power is required for voltage support, it occupies a portion of the inverter capacity, thereby reducing the available capacity for active power dispatch. As a result, the battery cannot fully exploit price arbitrage or reserve provision opportunities, and the resulting loss in revenue is reflected in the opportunity cost calculation. Specifically, the value of flexibility is defined as the difference in revenue between the unconstrained (market-driven) operation and the constrained (network-aware) operation, thereby directly quantifying the economic impact of technical constraints, including reactive power requirements.

Figures presented in this section visualize 24-h operation of the BSU across four representative days. Each figure includes the SOE, the charging and discharging activities, the PCR reserve commitment, the DA market prices, and reactive power provision (if applicable). SOE is plotted on the primary y-axis, DA prices on the secondary axis, and battery power activities are illustrated using the grouped bar charts. These plots highlight the BSU's flexibility in adapting to market signals and grid conditions.

The comparative results reveal consistent patterns: in unconstrained scenarios, the BSU follows the efficient charge/discharge strategies driven by price signals. It typically charges during the off-peak hours and discharges during the peak price periods. On the other hand, the PCR services are utilized whenever profitable. In contrast, in network-constrained scenarios the BSU is often required to provide reactive support, particularly in voltage-critical hours. This additional service reduces the room for arbitrage, alters the SOE profile, and flattens the energy activity throughout the day. The most pronounced deviation is observed on 3 July, where the BSU provides extensive reactive power, resulting in a visible decrease in arbitrage cycles and a profit drop of 2.07%. Other days, such as 5 April, show minimal deviation, with nearly identical profit values and operational strategies regardless of the constraints.

To assess the economic implications of these observations, the difference in profit between the unconstrained and the constrained scenarios is proposed as a flexibility fee, i.e., a value that quantifies the BSU's contribution to non-remunerated services such as voltage support. The studied BSU has a rated capacity of 13.7 MWh and 5 MW of charge/discharge power, with a capital cost of 3.425 million EUR (assuming 250,000 EUR/MWh investment cost). Based on the weighted frequency of representative days throughout the year, annual profits are calculated and summarized in Table 3. These values are consistent with the applied weighting factors and correspond to each representative cluster, which is represented by a specific day.

Table 3. BSU profit comparison with and without network constraints.

Date	No Consts [EUR]	With Consts [EUR]	Difference [EUR]	Loss [%]
3 July	161,259	157,914	−3345	2.07%
5 November	214,011	212,535	−1476	0.69%
5 April	931,180	930,754	−426	0.05%
26 February	310,028	309,585	−443	0.14%
Total per year	**1,616,478**	**1,610,788**	**−5690**	—

In the proposed framework, a set of representative days with assigned weight factors is used to approximate full-year operation while maintaining computational tractability. Within this representation, the profit gap due to network constraints amounts to 5690 EUR annually, which we define as the "annual flexibility fee." The four days shown in Table 3 represent typical operating conditions under network constraints and illustrate the economic impact of flexibility provision.

This corresponds to a relatively small reduction in annual profit, confirming that the economic impact of network constraints is limited but non-negligible. The results indicate

that, although network constraints slightly restrict market participation, the battery storage system retains most of its revenue-generating capability.

Under unconstrained operation, the BSU achieves an ROI of 47.03% with a payback period of 2.12 years. When constraints are included, ROI decreases to 38.14% and payback extends to 2.6 years. If the flexibility fee were formally awarded to the BSU operator, both ROI and payback would return to levels comparable to the unconstrained case. As shown in Table 4 for the observed year, the impact of network constraints is mainly reflected in reduced profitability due to limited operational flexibility, while the fundamental economic attractiveness of the BSU remains preserved. To gain even further insights into the impact of different representative days and the presence of technical constraints, Figure 9 illustrates BSU operational strategies across four representative days.

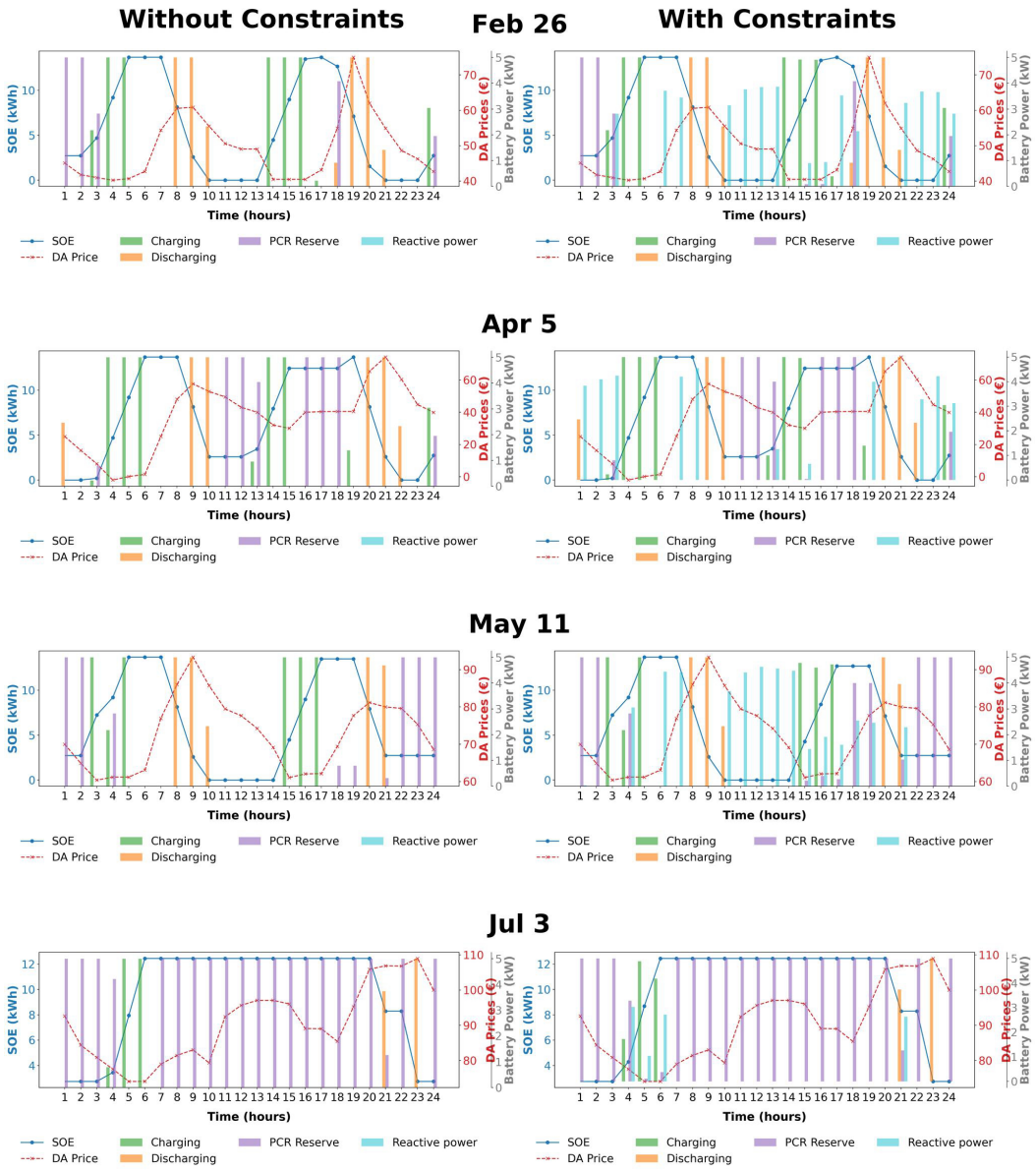


Figure 9. Comparison of the BSU operational strategies on four representative days (7 March, 11 May, 5 April, 26 February). Each row shows the battery activity across a 24-h period: the left column displays results without the network constraints, while the right column includes full AC network limitations. The figures display SOE (blue line), DA price (red dashed), charging power (green bars), discharging power (orange bars), PCR activities (purple bars), and reactive power (cyan bars).

Table 4. Return on investment (ROI) and payback time.

Scenario	ROI [%]	Payback Period [Years]
Without Network Constraints	47.03%	2.12
With Constraints (No Flex Fee)	38.14%	2.6
With Flexibility Fee Awarded	47.03%	2.12

These findings confirm the necessity of flexibility compensation schemes. Even in highly profitable projects, technical constraints shift a portion of the BSU's operational effort from market-oriented optimization to essential grid-support functions. Without proper incentives, this trade-off discourages storage deployment in critical network areas. Formal recognition of flexibility as a service—quantified by lost revenue in constrained conditions could unlock more resilient and economically viable storage-based grid architectures.

It is important to distinguish between the cumulative slack energy obtained from the infeasibility analysis and the energy capacity requirement of the battery storage system. The slack variables quantify the minimum instantaneous corrective action required to restore feasibility in the absence of storage, whereas the battery sizing problem enforces state-of-energy constraints over contiguous infeasible periods. As a result, the required battery energy capacity is driven by the need to guarantee sustained feasibility over long congestion blocks, rather than by the integral of slack values alone. Consequently, the optimized battery energy capacity may significantly exceed the cumulative slack energy observed in the infeasibility analysis, reflecting a robustness requirement rather than actual dispatched energy.

4. Conclusions

This paper addresses a significant challenge associated with the high penetration of renewable energy sources in power distribution networks. The increasing occurrence of local congestion and voltage violations represents a major barrier to further renewable integration and calls for cost-efficient alternatives to conventional network reinforcement. To this end, a practical and economically transparent framework is proposed in this work that enables DSOs to evaluate battery energy storage as a flexible non-wire solution. The paper introduces a relatively straightforward yet effective concept for incentivizing profit-oriented BSU operators to provide essential grid services while receiving appropriate compensation. The proposed framework supports DSOs in determining the most suitable strategy to ensure safe and reliable network operation, whether through traditional network expansion or through the procurement of flexibility from storage assets. Two complementary implementation pathways are identified: encouraging private investment in BSUs at congestion-prone locations identified by the DSO, and providing targeted incentives for storage deployment at locations that may not be attractive to private investors under purely energy-market-driven conditions. This approach closely mirrors real-world operational practice, where DSOs first identify critical network locations and subsequently initiate tendering or incentive-based mechanisms.

Furthermore, an algorithm for calculating the minimum economic value of flexibility is developed and demonstrated through a detailed case study. By explicitly quantifying flexibility as an opportunity cost arising from deviations from profit-maximizing battery operation, the proposed method serves as a decision-support tool for assessing whether congestion issues are more cost-effectively addressed through private investment, i.e., incentivized flexibility, or conventional grid reinforcement.

The findings of this paper are particularly relevant for distribution system operators and policymakers involved in the design of flexibility procurement mechanisms. The results demonstrate that battery energy storage systems can effectively eliminate voltage violations

and restore network feasibility with relatively limited economic impact, making them a viable non-wire alternative to traditional grid reinforcement. Furthermore, the proposed framework provides a transparent method for quantifying the value of flexibility based on opportunity cost, which can support the development of market-based procurement strategies and tender procedures. This is especially important in regulatory environments where DSOs are restricted from owning storage assets, as it enables economically justified interaction between network needs and market-driven battery operation.

Despite the practical relevance of the proposed framework, several limitations should be acknowledged. The analysis is based on a single distribution network topology and assumes perfect foresight of load profiles and market prices. Moreover, the battery model does not explicitly account for degradation effects, and uncertainty in renewable generation and demand is not considered. In addition, the optimization framework relies on a deterministic formulation and convex relaxations of the AC power flow equations, which, while ensuring tractability, may not fully capture all operational nonlinearities under extreme conditions. It should be noted that the magnitude of the economic impact of flexibility provision is highly dependent on system-specific conditions, such as renewable energy penetration, network characteristics, and market dynamics, while the primary contribution of this work lies in demonstrating a generalizable methodology for quantifying the value of flexibility.

Although the analysis is based on a single network and one year of data, the proposed methodology is general and can be applied to different distribution systems, operating conditions, and market environments. The magnitude of the obtained results depends on system-specific characteristics, such as renewable energy penetration, load profiles, and network topology; however, the framework itself provides a transferable approach for evaluating battery storage as a non-wire alternative and quantifying the value of flexibility.

Future research will therefore focus on extending the proposed framework along several dimensions. These include the incorporation of additional revenue streams, such as redispatch services provided to the transmission system operator, as well as the integration of battery degradation models and uncertainty-aware formulations. The application of more advanced optimization techniques, such as stochastic, robust, or decomposition-based methods, also represents a promising avenue for improving scalability and realism, particularly for large-scale or highly meshed distribution networks. Such extensions would further enhance the applicability of the proposed approach in the context of increasingly complex and renewable-dominated power systems.

Author Contributions: D.B.: Conceptualization, Methodology, Software, Formal analysis, Investigation, Writing—original draft, Visualization. H.P.: Supervision, Writing—review & editing. All authors have read and agreed to the published version of the manuscript.

Funding: The work is supported by the Croatian Science Foundation (HRZZ) under project Coordinated Hydrogen and Electricity SyStems and markets—CHESS (IP-2024-05-6299). The research was also funded by the European Union's NextGenerationEU programme, as part of the institutional project "Resilient Self-Healing Future Power Systems—RePowerFER," which is included in the programme agreement of the University of Zagreb Faculty of Electrical Engineering and Computing. The views and opinions expressed are solely those of the author and do not necessarily reflect the official position of the European Union or the European Commission. Neither the European Union nor the European Commission can be held responsible for them.

Data Availability Statement: The authors declare that all data supporting the findings of this study are available within the article or from the corresponding author upon reasonable request.

Conflicts of Interest: The authors declare no conflicts of interest.

References

1. Santamouris, M.; Vasilakopoulou, K. Present and future energy consumption of buildings: Challenges and opportunities towards decarbonisation. *e-Prime Adv. Electr. Eng. Electron. Energy* **2021**, *1*, 100002. [CrossRef]
2. Strezoski, L.; Padullaparti, H.; Ding, F.; Baggu, M. Integration of Utility Distributed Energy Resource Management System and Aggregators for Evolving Distribution System Operators. *J. Mod. Power Syst. Clean Energy* **2022**, *10*, 277–285. [CrossRef]
3. Sun, X.; Lin, L.; Wu, S.; Zhai, X.; Jin, C.; Pan, X. Comprehensive benefit assessment of photovoltaic and energy storage projects in incremental distribution networks under multiple coupled markets. *J. Energy Storage* **2025**, *133*, 117949. [CrossRef]
4. RePowerEU Plan. European Commission: Brussels, Belgium. Available online: https://eur-lex.europa.eu/legal-content/EN/TXT/?uri=COM%3A2022%3A230%3AFIN&qid=1653033742483 (accessed on 7 February 2023).
5. Croatian Electricity Market Act. Croatian Parliament: Zagreb, Croatia. Available online: https://www.zakon.hr/z/377/Zakon-o-tr%C5%BEi%C5%A1tu-elektri%C4%8Dne-energije (accessed on 7 February 2023).
6. Badanjak, D.; Pandžić, H. Interaction between the Distribution System Operator and the Battery Storage Operator for Flexibility Procurement Services. In Proceedings of the 2022 Power System and Green Energy Conference (PSGEC), Shanghai, China, 25–27 August 2022.
7. Fatima, S.; Puvi, V.; Lehtonen, M. Review on the PV Hosting Capacity in Distribution Networks. *Energies* **2020**, *13* , 4756. [CrossRef]
8. Pandžić, H.; Wang, Y.; Qiu, T.; Dvorkin, Y.; Kirschen, D.S. Near-Optimal Method for Siting and Sizing of Distributed Storage in a Transmission Network. *IEEE Trans. Power Syst.* **2015**, *30*, 2288–2300. [CrossRef]
9. Dimač, F.; Rajšl, I.; Raos, S. The Roles of Battery Energy Storage System in Different Energy Communities. *J. Energy Energ.* **2024**, *73*, 16–25.
10. Qamar, N.; Arshad, A.; Mahmoud, K.; Lehtonen, M. Hosting Capacity in Distribution Grids A Review of Definitions, Performance Indices, Determination Methodologies, and Enhancement Techniques. *Energy Sci. Eng.* **2023**, *11*, 1536–1559. [CrossRef]
11. Tuinema, B.W.; Torres, J.L.R.; Stefanov, A.I.; Gonzalez-Longatt, F.M.; Meijden, M.A.M.M.V. *Probabilistic Reliability Analysis of Power Systems*; Springer: Berlin/Heidelberg, Germany, 2020.
12. Ding, F.; Mather, B. On Distributed PV Hosting Capacity Estimation, Sensitivity Study and Improvement. In Proceedings of the IEEE Power & Energy Society General Meeting (PESGM), Portland, OR, USA, 5–10 August 2018.
13. Kamruzzaman, M.; Bhusal, N.; Benidris, M. Determining Maximum Hosting Capacity of Electric Distribution Systems to Electric Vehicles. In Proceedings of the IEEE Industry Applications Society Annual Meeting, Baltimore, MD, USA, 28 September–3 October 2019.
14. Zhang, L.; Ye, H.; Ding, F.; Li, Z.; Shahidehpour, M. Increasing PV Hosting Capacity with an Adjustable Hybrid Power Flow Model. *IEEE Trans. Sustain. Energy* **2023**, *14*, 409–422. [CrossRef]
15. Sahu, S.K.; Ghosh, D. Hosting Capacity Enhancement in Distribution System in Highly Trenchant Photo-Voltaic Environment: A Hardware in Loop Approach. *IEEE Access* **2020**, *8*, 14440–14451. [CrossRef]
16. Boonluk, P.; Siritaratiwat, A.; Fuangfoo, P.; Khunkiti, S. Optimal Siting and Sizing of Battery Energy Storage Systems for Distribution Network of Distribution System Operators. *Batteries* **2020**, *6*, 56. [CrossRef]
17. Gomes, C.A.M.; Ferreira, H.P. Hosting capacity evaluation of distributed generation systems with genetic algorithm. In Proceedings of the Simposio Brasileiro de Sistemas Eletricos (SBSE), Niteroi, Brazil, 12–16 May 2018.
18. Pandžić, K.; Pandžić, H.; Kuzle, I. Coordination of Regulated and Merchant Energy Storage Investments. *IEEE Trans. Sustain. Energy* **2018**, *9*, 1244–1254. [CrossRef]
19. Dvorkin, Y.; Fernandez-Blanco, R.; Wang, Y.; Xu, B.; Kirschen, D.S.; Pandžić, H.; Watson, J.-P.; Silva-Monroy, C.A. Co-Planning of Investments in Transmission and Merchant Energy Storage. *IEEE Trans. Power Syst.* **2018**, *33*, 245–256. [CrossRef]
20. Na, S.; Xumin, L.; Yong, G. Research on k-means Clustering Algorithm: An Improved k-means Clustering Algorithm. In Proceedings of the Third International Symposium on Intelligent Information Technology and Security Informatics, Jinggangshan, China, 2–4 April 2010.
21. Sharma, D.D.; Singh, S.N. Electrical load profile analysis and peak load assessment using clustering technique. In Proceedings of the 2014 IEEE PES General Meeting, National Harbor, MD, USA, 27–31 July 2014.
22. Jeong, H.C.; Jang, M.; Kim, T.; Joo, S.K. Clustering of Load Profiles of Residential Customers Using Extreme Points and Demographic Characteristics. *Electronics* **2021**, *10*, 290. [CrossRef]
23. McLoughlin, F.; Conlon, A.D.M. A clustering approach to domestic electricity load profile characterisation using smart metering data. *Appl. Energy* **2015**, *141*, 190–199. [CrossRef]
24. Azad, S.A.; Ali, A.B.M.S.; Wolfs, P. Identification of typical load profiles using K-means clustering algorithm. In Proceedings of the Asia-Pacific World Congress on Computer Science and Engineering, Nadi, Fiji, 4–5 November 2014.
25. Electricity Market Design. European Comission: Bruxelles, Belgium. Available online: https://energy.ec.europa.eu/topics/markets-and-consumers/electricity-market-design_en (accessed on 23 December 2025).

26. Basics of the Power Market. Epex Spot: Paris, France. Available online: https://www.epexspot.com/en/basicspowermarket (accessed on 23 December 2025).
27. Badanjak, D.; Pandžić, H. Distribution-Level Flexibility Markets—A Review of Trends, Research Projects, Key Stakeholders and Open Questions. *Energies* **2021**, *14*, 6622. [CrossRef]
28. Vicente-Pastor, A.; Nieto-Martin, J.; Bunn, D.W.; Laur, A. Evaluation of Flexibility Markets for Retailer–DSO–TSO Coordination. *IEEE Trans. Power Syst.* **2019**, *34*, 2003–2012. [CrossRef]
29. Bobanac, V.; Pandžić, H.; Bašić, H. Accurate Modeling of Lithium-ion Batteries for Power System Economics. *IEEE Trans. Power Syst.* **2025**, *40*, 1738–1750. [CrossRef]
30. Farivar, M.; Low, S.H. Branch flow model: Relaxations and Convexification—Part I. *IEEE Trans. Power Syst.* **2013**, *28*, 2554–2564. [CrossRef]
31. Farivar, M.; Low, S.H. Branch flow model: Relaxations and convexification—Part II. *IEEE Trans. Power Syst.* **2013**, *28*, 2565–2572. [CrossRef]
32. Molzahn, D.K.; Hiskens, I.A. A Survey of Relaxations and Approximations of the Power Flow Equations. In *Foundations and Trends in Electric Energy Systems*; Now Publishers Inc.: Hanover, MA, USA, 2019; Volume 4.
33. Pedregosa, F.; Varoquaux, G.; Gramfort, A.; Michel, V.; Thirion, B.; Grisel, O.; Blondel, M.; Prettenhofer, P.; Weiss, R.; Dubourg, V.; et al. Scikit-learn: Machine Learning in Python. *J. Mach. Learn. Res.* **2011**, *12*, 2825–2830.
34. Clustering, Scikit-Lear. Available online: https://scikit-learn.org/stable/modules/clustering.html#k-means (accessed on 7 February 2023).
35. Das, D.; Kothari, D.P.; Kalam, A. Simple and efficient method for load flow solution of radial distribution networks. *Electr. Power Energy Syst.* **1995**, *17*, 335–346. [CrossRef]
36. Croatian Power Exchange: Zagreb, Croatia. Available online: www.cropex.hr/en (accessed on 20 January 2023).
37. Croatian Energy Market Operator: Zagreb, Croatia. Available online: https://www.hrote.hr/en (accessed on 20 January 2023).
38. Statista: Hamburg, Germany. Available online: https://www.statista.com/statistics/1267500/eu-monthly-wholesale-electricity-price-country/#:~:text=In%202021%2C%20wholesale%20electricity%20prices,due%20to%20low%20wind%20speeds (accessed on 25 January 2023).
39. Elbow Method for Optimal Value of k in K-Means. GeeksforGeeks: Noida, India. Available online: https://www.geeksforgeeks.org/elbow-method-for-optimal-value-of-k-in-kmeans/ (accessed on 10 February 2023).

Disclaimer/Publisher's Note: The statements, opinions and data contained in all publications are solely those of the individual author(s) and contributor(s) and not of MDPI and/or the editor(s). MDPI and/or the editor(s) disclaim responsibility for any injury to people or property resulting from any ideas, methods, instructions or products referred to in the content.